

## Symmetry-adapted coupled-pair approach to the many-electron correlation problem. I. *LS*-adapted theory for closed-shell atoms

B. G. Adams

*Department of Chemistry, University of New Brunswick, Fredericton, N.B., E3B 6E2, Canada*

J. Paldus\*

*Quantum Theory Group, Department of Applied Mathematics, University of Waterloo, Waterloo, Ontario, N2L 3G1, Canada*

(Received 26 November 1980)

The orthogonally spin- and orbital-symmetry-adapted (*LS*-coupled) coupled-pair many-electron theory and its extended version involving monoexcited and biexcited cluster coefficients is derived in a form suitable for application to closed-shell atomic systems. A diagrammatic approach, based on second quantization, the time-independent Wick theorem, and the graphical methods of spin algebras, is employed.

### I. INTRODUCTION

Recently there has been a renewed interest in coupled-cluster approaches<sup>1,2</sup> and a number of actual applications have been carried out.<sup>3-5</sup> This approach exploits the logarithm of the wave operator and formulates equations which determine its components. Basically these equations represent recursion formulas for the generation of the relevant diagrams of MBPT, which are then automatically summed to infinite order by solving the equations. The idea of using the cluster expansion was first suggested in nuclear correlation problems by Coster and Kummel<sup>1</sup> and the general equations for the calculations of cluster components were given by Čížek.<sup>2</sup> A number of alternative derivations have since been given<sup>6,7</sup> and a number of extensive expositions are now available.<sup>8-11</sup> A brief overview of the various motivations, origins and developments of this approach has also been given, recently.<sup>12</sup>

We have previously derived the orthogonally spin-adapted version of the coupled-pair many-electron theory<sup>13</sup> (CPMET) and its extended version<sup>14</sup> (ECPMET) including triexcited clusters by combining the time-independent diagrammatic techniques<sup>2,15</sup> with the graphical methods of spin algebras.<sup>11,15-20</sup> We have also discussed the advantages of this orthogonally spin-adapted version,<sup>14</sup> which is based essentially on the hole-particle Gelfand states<sup>21</sup> over the standard CPMET<sup>2</sup> and ECPMET<sup>22</sup> versions which are based on non-orthogonal spin-bonded functions.

In applications to actual systems we can often exploit in addition to the spin symmetry (implied by the spin independence of the Hamiltonian), various other symmetries, which leave the Hamiltonian invariant, particularly the point group spatial symmetries. The latter are especially important

in applications to atomic systems whose Hamiltonian is invariant under the operations of the three-dimensional rotation group. In fact, in this case the angular dependence can be completely eliminated from the coupled-pair (or, generally, coupled-cluster) equations to obtain radial coupled-pair equations,<sup>5,11</sup> which can be solved numerically using an iterative self-consistent scheme.<sup>5,23-25</sup>

In this paper we present the orthogonally spin- and angular momentum adapted CPMET equations for the case of closed-shell atomic systems using an analytical form for the intervening wave functions. It is well known, at least currently, that the analytic approach is the only feasible one in the case of molecular systems. In this approach the one-electron (molecular) orbital states are expanded in terms of a finite one-electron basis, usually consisting of Gaussian- or Slater-type atomic orbitals, localized on various nuclei of the molecular system. Moreover, this approach has proven to be useful even for central atomic systems in both Hartree-Fock<sup>26,27</sup> (HF) and correlation energy<sup>28</sup> studies. Such systems can also serve as an excellent testing ground for various approximate approaches to the correlation problem which are primarily intended for applications to molecular systems.

The results and analysis of the application of the spin- and angular momentum adapted CPMET equations given in this paper to the Be atom and several CEPA-type approximations to CPMET will be presented in subsequent papers.<sup>29</sup>

### II. REVIEW OF COUPLED-CLUSTER FORMALISM

We briefly review our notation and formalism for the coupled-cluster theory.<sup>2,13,14</sup> Let  $|\Psi\rangle$  and  $|\Phi\rangle$  be the exact- and independent-particle-model

nonrelativistic ground-state wave functions, respectively, of an  $N(=2n)$  electron closed-shell system described by a spin-independent Hamiltonian  $H$  whose normal product form  $H_N$  is defined in terms of an orthonormal set  $\{|A\rangle\}$  of spin orbitals, and the corresponding sets of annihilation  $\{X_A\}$  and creation  $\{X_A^\dagger\}$  operators, by<sup>2,15</sup>

$$H_N = H - \langle \Phi | H | \Phi \rangle = F_N + V_N, \quad (2.1)$$

where

$$F_N = \sum_{AB} \langle A | f | B \rangle N[X_A^\dagger X_B], \quad (2.2)$$

$$V_N = \frac{1}{2} \sum_{ABCD} \langle AB | v | CD \rangle N[X_A^\dagger X_B^\dagger X_D X_C], \quad (2.3)$$

and  $N[\dots]$  indicates the normal product ordering<sup>15</sup> with respect to  $|\Phi\rangle$ . The one-electron matrix elements in (2.2) are given by

$$\langle A | f | B \rangle = \langle A | z | B \rangle + \sum_{C_1} \langle AC_1 | v | BC_1 \rangle_A, \quad (2.4)$$

where

$$\langle AB | v | CD \rangle_A = \langle AB | v | CD \rangle - \langle AB | v | DC \rangle. \quad (2.5)$$

If  $|\Phi\rangle$  is the HF ground state then  $f$  is just the one-electron Fock operator and  $\langle A | f | B \rangle = \epsilon_A \delta_{AB}$ , where each  $\epsilon_A$  is an HF orbital energy. For atomic systems, using Hartree atomic units, the operators  $z$  and  $v$  are defined as

$$z(\vec{r}_i) = -\frac{1}{2} \Delta_i - \frac{Z}{r_i}, \quad (2.6)$$

$$v(\vec{r}_i, \vec{r}_j) = 1/|\vec{r}_i - \vec{r}_j|, \quad (2.7)$$

in terms of the Laplacian  $\Delta_i$ , position vector  $\vec{r}_i$  of length  $r_i = |\vec{r}_i|$  for electron  $i$ , and the nuclear charge  $Z$ .

In the above equations we are using the following notation<sup>13,14</sup>: capital (lower) case latin letters label spin orbitals (orbitals), lower case Greek letters label spin functions, *numerical* superscripts (subscripts) refer to particles (holes), and labels without indices or with *nonnumerical* indices [e.g., in (3.8) below] refer to arbitrary one-electron functions. Thus, for example, the sum in (2.4) extends over all hole states (i.e., those occupied in  $|\Phi\rangle$ ).

The normal product form of the Schrödinger equation is

$$H_N |\Psi\rangle = \Delta\epsilon |\Psi\rangle, \quad (2.8)$$

where  $\Delta\epsilon$  is the correlation energy, relative to  $|\Phi\rangle$ , given in terms of the exact ground-state energy eigenvalue  $E$  of  $H$  by

$$\Delta\epsilon = E - \langle \Phi | H | \Phi \rangle = \langle \Phi | H_N | \Psi \rangle, \quad (2.9)$$

where the latter expression, which is used in the coupled-cluster theory, is obtained by imposing the intermediate normalization condition

$$\langle \Phi | \Psi \rangle = 1 (= \langle \Phi | \Phi \rangle). \quad (2.10)$$

In the closed-shell coupled-cluster approach the exact wave function  $|\Psi\rangle$  is expressed in terms of  $|\Phi\rangle$ , and the monoexcited, biexcited, etc., excited configurations obtained from  $|\Phi\rangle$ , via the cluster expansion

$$|\Psi\rangle = e^T |\Phi\rangle, \quad (2.11a)$$

where

$$T = \sum_{i=1}^N T_i \quad (2.11b)$$

is a sum of  $i$ -fold excitation operators which can be expressed as

$$T_i = (i!)^{-2} \sum_{\{B\}} \langle B^1 \dots B^i | t_i | B_1 \dots B_i \rangle_A \prod_{j=1}^i X_{B_j}^\dagger X_{B_j}, \quad (2.12)$$

in terms of fully antisymmetrized  $t_i$  cluster coefficients (matrix elements).<sup>2,13,14</sup> Using (2.11) in (2.8) and diagrammatic methods based on second quantization and the *time-independent* generalized Wick theorem<sup>15</sup> we easily obtain the linked-cluster form

$$(H_N e^T)_c |\Phi\rangle = \Delta\epsilon |\Phi\rangle \quad (2.13)$$

of the Schrödinger Eq. (2.8), where the subscript  $c$  refers to connected diagrams only. The various approximations such as CPMET ( $T \approx T_2$ )<sup>2</sup> are then obtained by projecting (2.13) onto the appropriate set of configurations (the biexcited ones for CPMET).<sup>13,14</sup> For the spin-orbital version of the theory these are just the usual  $i$ -fold excited configurations [cf. Eq. (3.1) of Ref. 14]. In particular, the correlation energy is given by<sup>2</sup>

$$\Delta\epsilon = \langle \Phi | (H_N e^T)_c | \Phi \rangle, \quad (2.14)$$

and the remaining equations, which do not contain the correlation energy, provide a system of coupled nonlinear algebraic equations determining the various cluster coefficients.

We have previously mentioned<sup>13,14</sup> that it is very convenient to choose orthogonal symmetry-adapted states and cluster coefficients for this purpose and we have recently carried out this procedure for CPMET<sup>13</sup> and a version of ECPMET involving monoexcited, biexcited and triexcited states,<sup>14</sup> using orthogonal spin-adapted states and cluster coefficients. In this paper we derive the CPMET equations and the equations for a version of ECPMET with  $T \approx T_1 + T_2$ , in a form suitable for application to closed-shell atomic systems, by projecting (2.13) onto a suitable set of spin- and

angular momentum adapted (*LS*-coupled) states. First, however, we shall introduce the notation and conventions which we shall need in the case of atomic systems.

### III. NOTATION AND CONVENTIONS FOR ATOMIC SYSTEMS

For atoms the spin orbitals can be expressed as

$$|A\rangle = |a\rangle |\alpha\rangle = |n_a l_a m_a\rangle |\alpha\rangle, \quad (3.1)$$

where  $|\alpha\rangle$  is one of the orthonormal spin functions  $|\pm\frac{1}{2}\rangle$  and  $|a\rangle$  is an atomic orbital defined by the magnetic quantum number  $m_a$ , the orbital angular momentum quantum number  $l_a$ , and the  $l_a$ -dependent quantum number  $n_a$  which enumerates the various atomic shells ( $n_a l_a$ ). A finite set of atomic orbitals can thus, for example, be defined in the usual spherical coordinate system by

$$\phi_{nlm}(r, \theta, \phi) = R_{nl}(r) Y_{lm}(\theta, \phi), \quad (3.2)$$

where  $l=0, 1, \dots, l_{\max}$ ,  $n=1, 2, \dots, N(l)$ , the angular functions  $Y_{lm}$  are the usual spherical harmonics<sup>30</sup> and the radial functions satisfy the orthogonality relations

$$\int_0^\infty R_{n'l'}^*(r) R_{nl}(r) r^2 dr = \delta(n', n) \delta(l', l) \quad (3.3)$$

which guarantee that  $\{\phi_{nlm}\}$  is an orthonormal set of atomic orbitals. In the analytical approach, which we are using, the radial functions for occupied orbitals are commonly chosen as approximate variationally determined solutions of the radial HF equations<sup>31</sup> and are expressed as linear com-

binations of Slater-type radial functions.<sup>32</sup> The radial functions for unoccupied (virtual) orbitals are then chosen to satisfy (3.3) with respect to each other and to the occupied orbitals. This latter requirement can be automatically satisfied by choosing virtual HF radial functions although this is by no means necessary. Thus, in the analytical approach, the first step is to express the  $f$  and  $v$  matrix elements in (2.2) and (2.3) in terms of integrals involving the radial functions.

#### A. Factorization of one- and two-electron matrix elements

For atomic systems the factorization of the  $f$  and  $v$  matrix elements into their spin, angular momentum, and radial parts, using (2.6), (2.7), and (3.2), is well known and can be accomplished in several ways. The classical approach<sup>32</sup> does not use the more powerful methods of angular momentum theory and tensor operators.<sup>20, 33</sup> This latter approach can be combined with the graphical methods of spin algebras<sup>11, 16-20, 34</sup> to provide a very simple derivation and graphical representation of the results. Since we shall be using these graphical methods extensively in the following, we briefly summarize the results in order to fix our notations, conventions, and graphical representations.

The spin dependence of the  $f$  and  $v$  matrix elements is trivial, and the orbital  $v$  matrix elements can now be factorized into their angular and radial parts by using the tensor-operator expansion of the two-electron interaction (2.7).<sup>33</sup> The final result is

$$\langle ab | v | cd \rangle = \langle ac | v | bd \rangle = \sum_{k=0}^{k_{\max}} A^k(l_a m_a l_c m_c | l_b m_b l_d m_d) X^k(n_a l_a n_c l_c | n_b l_b n_d l_d), \quad (3.4)$$

where

$$A^k(l_a m_a l_c m_c | l_b m_b l_d m_d) = \sum_{q=-k}^k \begin{pmatrix} l_a & q & m_c \\ m_a & k & l_c \end{pmatrix} \begin{pmatrix} l_b & k & m_d \\ m_b & q & l_d \end{pmatrix} \quad (3.5)$$

and the radial integral  $X^k$  is given by

$$X^k(n_a l_a n_c l_c | n_b l_b n_d l_d) = C^k(l_a l_c | l_b l_d) R^k(n_a l_a n_c l_c | n_b l_b n_d l_d), \quad (3.6)$$

in terms of the angular coefficient

$$C^k(l_a l_c | l_b l_d) = (-1)^k \langle l_a || C^k || l_c \rangle \langle l_b || C^k || l_d \rangle \quad (3.7)$$

and the radial integral

$$R^k(n_a l_a n_c l_c | n_b l_b n_d l_d) = \int_0^\infty r_1^2 dr_1 \int_0^\infty r_2^2 dr_2 v^k(r_1, r_2) R_{n_a l_a}^*(r_1) R_{n_c l_c}(r_1) R_{n_b l_b}^*(r_2) R_{n_d l_d}(r_2), \quad (3.8)$$

where

$$v^k(r_1, r_2) = \begin{cases} r_1^k / r_2^{k+1}, & r_1 \leq r_2 \\ r_2^k / r_1^{k+1}, & r_1 > r_2 \end{cases} \quad (3.9)$$

In (3.5) we are using Wigner's form<sup>17, 35</sup> of the 3- $jm$  symbol and in (3.7) the reduced matrix elements of the tensor operator  $C^k$ , whose components are the Racah spherical harmonics

$$C_q^k(\theta, \phi) = (4\pi/[k])^{1/2} Y_{kq}(\theta, \phi), \quad (3.10)$$

and are defined using the convention of Refs. 17 and 35 for the Wigner-Eckart theorem. They are simply related to a special 3- $j$ m symbol:

$$\langle l \| C^k \| l' \rangle = (-1)^l [l, l']^{1/2} \begin{pmatrix} l & k & l' \\ 0 & 0 & 0 \end{pmatrix}. \quad (3.11)$$

In (3.10) and (3.11) and in the following we are using the compact Wigner notation<sup>35</sup>:

$$\begin{aligned} [l] &\equiv 2l + 1, \\ [l, l', \dots] &= [l][l'], \dots, \end{aligned} \quad (3.12)$$

A simple closed form expression for the 3- $j$ m symbol in (3.11) can easily be obtained.<sup>17</sup>

For the one-electron orbital  $z$  and  $f$  matrix elements we easily obtain the expressions

$$\begin{aligned} \langle a | z | b \rangle &= \delta(l_a, l_b) \delta(m_a, m_b) \langle n_a l_a | z | n_b l_b \rangle, \quad (3.13) \\ \langle a | f | b \rangle &= \delta(l_a, l_b) \delta(m_a, m_b) \langle n_a l_a | f | n_b l_b \rangle, \quad (3.14) \end{aligned}$$

in terms of the radial  $z$  and  $f$  matrix elements

$$\langle n_a l | z | n_b l \rangle = \int_0^\infty R_{n_a l}^*(r) [z_l(r) R_{n_b l}(r)] r^2 dr, \quad (3.15)$$

$$\begin{aligned} \langle n_a l | f | n_b l \rangle &= \langle n_a l | z | n_b l \rangle \\ &+ 2[l]^{-1/2} \sum_{n_1 l_1} [l_1]^{1/2} X^0(n_a l n_b l | n_1 l_1 n_1 l_1) \\ &- [l]^{-1} \sum_k \sum_{n_1 l_1} X^k(n_a l n_1 l_1 | n_1 l_1 n_b l), \end{aligned} \quad (3.16)$$

where

$$z_l(r) = \frac{1}{r} \left( -\frac{1}{2} \frac{d^2}{dr^2} + \frac{l(l+1)}{r^2} \right) r - \frac{Z}{r} \quad (3.17)$$

is the radial part of the operator  $z$  in (2.6). As mentioned above, (3.16) is most easily obtained using graphical methods. The practical calculation of the radial integrals in terms of their expansions involving Slater-type radial integrals is well known<sup>26</sup> and will not be summarized here.

#### B. Graphical representation of interaction vertices

We now consider the graphical representation of the Goldstone form of the  $F$  and  $V$  vertices corresponding to (2.2) and (2.3), respectively (cf. Fig. 1 of Ref. 13), which we shall need in the construction of the orbital angular momentum diagrams for the spin- and angular momentum adapted form of coupled-cluster theory for atomic systems (Sec. V), using the graphical methods of spin algebras<sup>11, 16-20</sup> and the formulas (3.14), (3.16), and (3.4) for the orbital  $f$  and  $v$  matrix elements.

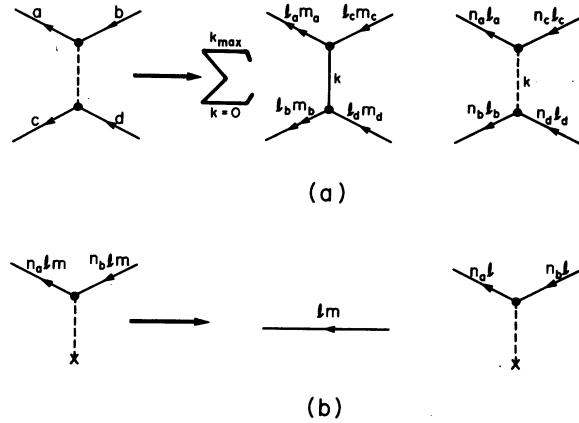


FIG. 1. Graphical representation of the orbital part of the Goldstone  $V$  vertex (a) corresponding to Eq. (3.4), and  $F$  vertex (b) corresponding to Eq. (3.14), for atomic systems (cf. Sec. III B of text for further details).

Each of the 3- $j$ m symbols in (3.5) can be represented graphically [cf. Eq. (58') of Ref. 18], and by using the summation rule (65) of Ref. 13 over the magnetic quantum number  $q$  we obtain, for the coefficient  $A^k$  appearing in (3.4), the first diagram of the right-hand side in Fig. 1(a). The vertex signs and the arrow on line  $k$  can be omitted.<sup>36</sup> The second diagram on the right-hand side in Fig. 1(a) represents the radial integral  $X^k$  defined in (3.6). We also note that the diagram representing  $A^k$  is topologically equivalent to the Goldstone  $V$  vertex. Thus, Fig. 1(a) represents the complete factorization of the orbital part of the Goldstone  $V$  vertex, which will be used in Sec. V for the construction of the orbital angular momentum diagrams arising in the coupled-cluster theory. The analogous results for the  $F$  vertex are trivial since the orbital  $f$  matrix element (3.14) is diagonal in the  $l$  and  $m$  quantum numbers and hence we obtain the trivial factorization given in Fig. 1(b), where the radial part corresponds to the radial matrix element (3.16).

#### IV. $LS$ -COUPLED STATES AND CLUSTER COEFFICIENTS

We now construct the orthonormal spin and angular momentum adapted ( $LS$ -coupled) states, onto which we project the Schrödinger Eq. (2.13) to obtain the coupled-cluster equations, using angular momentum theory and following closely Sec. III of Ref. 14, where the spin-adapted states and cluster coefficients were considered. The  $LS$ -coupled-cluster coefficients are then constructed in the same manner as the corresponding states. Finally, the graphical methods of spin algebras are used to construct the orbital angular momentum

diagrams representing the angular part of the  $LS$ -coupled states and cluster coefficients. These results, and the interaction diagrams of Fig. 1, are used in the next section to construct the orbital angular momentum diagrams associated with the orbital diagrams of the coupled-cluster theory.

#### A. $LS$ -coupled states

In the spin-adaptation process<sup>18</sup> it is convenient to use the hole-particle formalism with the hole-particle creation operators defined as

$$Y_{n_1 l_1 m_1 \beta_1}^\dagger = (-1)^{l_1 - m_1} (-1)^{1/2 - \beta_1} X_{n_1 l_1 \bar{m}_1 \bar{\beta}_1}, \quad (4.1)$$

$$Y_{n_1 l_1 m_1 \beta_1}^\dagger = X_{n_1 l_1 m_1 \beta_1}^\dagger, \quad (4.2)$$

where  $\bar{m}_1 = -m_1$ ,  $\bar{\beta}_1 = -\beta_1$ . The corresponding results for the annihilation operators can be obtained by Hermitian conjugation. The spin-symmetry-

adapted states are

$$\left[ \begin{array}{c} (nlm)^{1\dots i} \\ (nlm)_{1\dots i} \end{array} \right]_{X_S}^{SM_S} \quad (4.3)$$

$$= \left( \prod_{j=1}^i (-1)^{l_j - m_j} \right) \left[ \begin{array}{c} (nlm)^{1\dots i} \\ (nl\bar{m})_{1\dots i} \end{array} \right]_{X_S}^{SM_S},$$

where  $(nlm)^{1\dots i} = n^1 l^1 m^1 \dots n^i l^i m^i$ , etc. The states on the right-hand side are defined in Eq. (3.3) of Ref. 14 with  $b^j = n^j l^j m^j$ ,  $b_j = n_j l_j \bar{m}_j$ ,  $j = 1, \dots, i$ . The states on the left-hand side can be coupled in the usual way, using Clebsch-Gordan (CG) coefficients of the same type for the orbital angular momentum couplings as for the spin couplings (cf. Sec. III of Ref. 14). Thus, we obtain the  $LS$ -coupled states (eigenfunctions of  $L^2$ ,  $L_z$ ,  $S^2$ ,  $S_z$ )

$$\left[ \begin{array}{c} (nl)^{1\dots i} \\ (nl)_{1\dots i} \end{array} \right]_{X_L X_S}^{LM_L SM_S} = \sum_{\{m\}} [X_L X^L \{lm\} M_L] \left[ \begin{array}{c} (nlm)^{1\dots i} \\ (nlm)_{1\dots i} \end{array} \right]_{X_S}^{SM_S} \quad (4.4a)$$

$$= \sum_{\{m\}} \langle X_L X^L \{lm\} M_L \rangle \left[ \begin{array}{c} (nlm)^{1\dots i} \\ (nlm)_{1\dots i} \end{array} \right]_{X_S}^{SM_S}. \quad (4.4b)$$

The coefficient in (4.4a) is a generalized CG coefficient obtained as a product of the usual CG coefficients of  $SU(2)$  in terms of the chosen coupling scheme (cf. Sec. IIIA of Ref. 14). The labels  $X_L, X^L$  ( $X_S, X^S$ ) denote the sets of intermediate orbital angular momentum (spin) quantum numbers defining the coupling schemes for the hole  $X_L$  ( $X_S$ ) and particle  $X^L$  ( $X^S$ ) orbitals, respectively, and the summation extends over the set  $\{m\}$  of magnetic quantum numbers  $m_1, \dots, m_i, m^1, \dots, m^i$ , and the intermediate ones associated with  $X_L$  and  $X^L$ . The expression (4.4b) is needed for the graphical representation of the  $LS$ -coupled states. The states on the right-hand side of (4.4b) are obtained from those on the right-hand side of (4.3) by replacing  $\bar{m}_j$  with  $m_j$ ,  $j = 1, \dots, i$ , and the coefficients in (4.4b) are

$$\langle X_L X^L \{lm\} M_L \rangle = \left( \prod_{j=1}^i (-1)^{l_j + m_j} \right) [X_L X^L \{lm\} M_L] \quad (4.5)$$

and can be written in terms of CG coefficients without  $m$ -dependent phase factors [cf. Eq. (4.8) below].

If we define

$$d_2 = \langle l_2 m_2 l_1 m_1 | L_{12} M_{12} \rangle \langle l^1 m^1 l^2 m^2 | L^{12} M^{12} \rangle, \quad (4.6)$$

then the coefficients for the monoexcited and biexcited  $LS$ -coupled states, using  $pp$ - $hh$  coupling<sup>18</sup> are

$$[\{lm\} M_L] = \langle l_1 m_1 l^1 m^1 | M_L \rangle, \quad (4.7a)$$

$$[L_{12} L^{12} \{lm\} M_L] = d_2 \langle L_{12} m_{12} L^{12} m^{12} | M_L \rangle, \quad (4.7b)$$

corresponding to (3.5a) and (3.5b) of Ref. 14, and

$$\langle \{lm\} M_L \rangle = ([L]/[L^1])^{1/2} \langle LM_L l_1 m_1 | l^1 m^1 \rangle, \quad (4.8a)$$

$$\langle L_{12} L^{12} \{lm\} M_L \rangle = d_2 ([L]/[L^{12}])^{1/2} \langle LM_L L_{12} m_{12} | L^{12} m^{12} \rangle, \quad (4.8b)$$

corresponding to (3.6a) and (3.6b) of Ref. 14. Thus, we obtain the monoexcited and biexcited  $LS$ -coupled states

$$\left[ \begin{array}{c} n^1 l^1 \\ n_1 l_1 \end{array} \right]_{LM_L SM_S} = \sum_{\{m\}} \langle \{lm\} M_L \rangle \left[ \begin{array}{c} n^1 l^1 m^1 \\ n_1 l_1 m_1 \end{array} \right]_{SM_S}, \quad (4.9a)$$

$$\left| \begin{matrix} (nl)^{12} \\ (nl)_{12} \end{matrix} \right\rangle_{LM_L SM_S}^{L^{12} S^{12}} = \sum_{\{m\}} \langle L_{12} L^{12} \{lm\} LM_L \rangle \left| \begin{matrix} (nlm)^{12} \\ (nlm)_{12} \end{matrix} \right\rangle_{SM_S}^{X^S} \quad (4.9b)$$

For the closed-shell coupled-cluster theory we need only consider the singlet  $S$  states ( $L=S=0$ ) in which case  $L_{12}=L^{12}=L_i$ ,  $S_{12}=S^{12}=S_i$ , and we define the orthonormal  $LS$ -coupled states

$$\left| \begin{matrix} n^1 l^1 \\ n_1 l_1 \end{matrix} \right\rangle \equiv \left| \begin{matrix} n^1 l^1 \\ n_1 l_1 \end{matrix} \right\rangle_{0000}, \quad l^1 = l_1 \quad (4.10a)$$

$$\left| \begin{matrix} (nl)^{12} \\ (nl)_{12} \end{matrix} \right\rangle_{L_i S_i} \equiv \left| \begin{matrix} (nl)^{12} \\ (nl)_{12} \end{matrix} \right\rangle_{L_i S_i}^{0000}, \quad (4.10b)$$

which we shall use in the following section to obtain the  $LS$ -coupled form of the coupled-cluster equations. They represent the angular momentum symmetry adapted version of the spin-symmetry-adapted states defined by Eqs. (3.9a) and (3.9b) of Ref. 14. The symmetry properties of the states (4.10b) are given by

$$\left| \begin{matrix} (nl)^{\bar{\kappa}\kappa} \\ (nl)^{\bar{\lambda}\lambda} \end{matrix} \right\rangle_{L_i S_i} = \phi_P \phi_L \phi_S \left| \begin{matrix} (nl)^{12} \\ (nl)_{12} \end{matrix} \right\rangle_{L_i S_i}, \quad (4.11)$$

#### B. $LS$ -coupled-cluster coefficients

If we write the  $i$ -fold excited  $LS$ -coupled-cluster component of the wave function [cf. Eq. (2.12)] in the form

$$T_i |\Phi\rangle = \sum_{LM_L} \sum_{SM_S} T_i(LM_L SM_S) |\Phi\rangle \quad (4.15)$$

[cf. Eq. (3.27) of Ref. 14] then the  $LS$ -coupled-cluster components are defined by

$$T_i(LM_L SM_S) |\Phi\rangle = (i!)^{-2} \sum_{\{n\}} \sum_{X_L X^L} \sum_{X_S X^S} N_{ni}^{-2} \langle (nl)^{1 \dots i} | t_i(LM_L SM_S) | (nl)_{1 \dots i} \rangle_{X_L X^L X_S X^S} \left| \begin{matrix} (nl)^{1 \dots i} \\ (nl)_{1 \dots i} \end{matrix} \right\rangle_{LM_L SM_S}^{X^L X^S},$$

in terms of the  $LS$ -coupled states (4.4) and  $t_i$  cluster coefficients, where  $\{nl\}$  denotes the independent  $i$ -fold summation over all shells and  $N_{ni}$  is an appropriate normalization factor [Eq. (3.11) of Ref. 14]. Using the notation of (4.10) the singlet monoexcited and biexcited cluster components are

$$T_1(0000) |\Phi\rangle = \sum_{\{n\}} \langle n^1 l^1 | t_1(0) | n_1 l_1 \rangle \left| \begin{matrix} n^1 l^1 \\ n_1 l_1 \end{matrix} \right\rangle, \quad (4.17a)$$

$$T_2(0000) |\Phi\rangle = (2!)^{-2} \sum_{\{n\}} \sum_{L_i} \sum_{S_i} N_{ni}^{-2} \langle (nl)^{12} | t_2(L_i S_i) | (nl)_{12} \rangle \left| \begin{matrix} (nl)^{12} \\ (nl)_{12} \end{matrix} \right\rangle_{L_i S_i}, \quad (4.17b)$$

where, using a similar notation as in (4.10b),

$$\langle (nl)^{12} | t_2(L_i S_i) | (nl)_{12} \rangle \equiv \langle (nl)^{12} | t_2(0000) | (nl)_{12} \rangle_{L_i S_i}^{L_i S_i}, \quad (4.17c)$$

where the normalization factor  $N_{ni}$  is defined in Eq. (3.11) of Ref. 14 with  $b^j = n^j l^j$ ,  $b_j = n_j l_j$ ,  $j=1, 2$ . The  $LS$ -coupled singlet  $t_1$  and  $t_2$  cluster coefficients are defined in terms of the spin-symmetry-adapted coefficients by analogy with the result (4.9) for states. Thus,

$$\langle n^1 l^1 | t_1(0) | n_1 l_1 \rangle = \sum_{\{m\}} \langle \{lm\} 00 \rangle \langle n^1 l^1 m^1 | t_1(0) | n_1 l_1 m_1 \rangle, \quad (4.18a)$$

where

$$\kappa, \lambda = 1, 2 (\bar{1} = 2, \bar{2} = 1) \quad (4.12)$$

and the phase factors are

$$\phi_P = (-1)^{\kappa + \lambda}, \quad (4.13a)$$

$$\phi_L = (-1)^{\kappa \phi^{12} + \lambda \phi_{12}}, \quad (4.13b)$$

$$\phi_S = (-1)^{(\kappa + \lambda)(1 + S_i)}, \quad (4.13c)$$

where

$$\phi_{12} = l_1 + l_2 + L_i, \quad \phi^{12} = l^1 + l^2 + L_i. \quad (4.14)$$

The phase factors  $\phi_X$ ,  $X=P, L, S$  arise from the permutational symmetry of the basic Slater determinants [cf. Eq. (3.1) of Ref. 14], the orbital angular momentum symmetry, and the spin symmetry, respectively (cf. Sec. III C of Ref. 14 for a discussion of  $\phi_P$  and  $\phi_S$ ). Finally, we note that other coupling schemes, such as the ph-ph one, give rise to more complicated symmetry properties (cf. Ref. 18).

$$\langle (nl)^{12} | t_2(L_i S_i) | (nl)_{12} \rangle = \sum_{\{m\}} \langle L_i L_i \{lm\} 00 \rangle \langle (nlm)^{12} | t_2(S_i) | (nlm)_{12} \rangle, \quad (4.18b)$$

where the spin-symmetry-adapted cluster coefficients on the right-hand side in (4.18) are defined in Eq. (3.29) of Ref. 14 in terms of the appropriate spin orbital cluster coefficients, and the angular momentum coefficients are obtained from the singlet case of (4.8). By analogy with (4.11) we obtain the symmetry properties

$$\langle (nl)^{\bar{\kappa}\kappa} | t_2(L_i S_i) | (nl)_{\bar{\lambda}\lambda} \rangle = \phi_P \phi_L \phi_S \langle (nl)^{12} | t_2(L_i S_i) | (nl)_{12} \rangle. \quad (4.19)$$

Finally, in order to simplify the final form of the coupled-pair equations, we shall use the unnormalized biexcited states and cluster coefficients [denoted by  $\tau_2$  rather than  $t_2$ , and defined in Eq. (3.31a) of Ref. 14].

### C. Graphical representations

We now consider the graphical representation of the  $LS$ -coupled biexcited states and cluster coefficients, using the rules and terminology outlined in Refs. 2 and 13–15. The orbital diagram given in Fig. 2(a) is used either to represent the biexcited ket state (4.10b) or, in our case, the corresponding cluster coefficient or component (4.18b) and (4.17b). Diagrams of this type have been previously referred to as Brandow's form of Hugenholtz diagrams, or simply as Brandow diagrams, and we refer to Refs. 13 and 14 for further details. The labels used on the diagram of Fig. 2(a) define the cluster coefficient (4.18b) to be associated with the diagram. The spin and angular parts of the states or cluster coefficients will then be represented by the usual angular momentum diagrams. The spin diagrams for the monoexcited and biexcited states have been given elsewhere,<sup>13,18</sup> while the orbital angular momentum diagram is

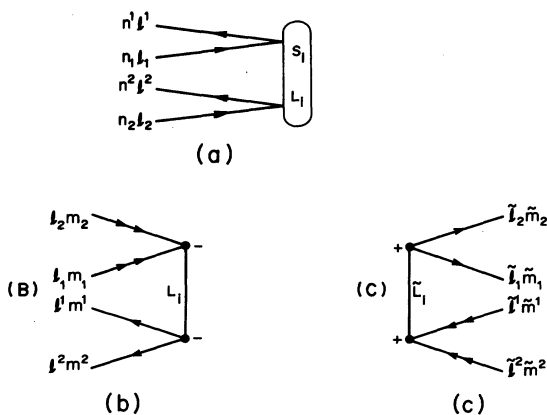


FIG. 2. Orbital (radial) Brandow diagram for the  $LS$ -coupled biexcited ket state or cluster coefficient (a) of Eq. (4.10b) or Eq. (4.18b), respectively, and the corresponding orbital angular momentum diagram (b) (cf. Sec. IV for further details); (c) is the orbital angular momentum diagram for the bra state appearing in Eq. (5.2b). The overall factors  $B$ ,  $C$  are given by  $B = [L_i]^{1/2}$ ,  $C = [\bar{L}_i]^{1/2}$ .

given in Fig. 2(b) for the  $LS$ -coupled biexcited state (4.10b) or equivalently, the cluster coefficient (4.18b). The corresponding result for the bra state is given in Fig. 2(c) (cf. Sec. V). Thus, in the construction of the orbital angular momentum diagrams of CPMET, Fig. 2(b) is used for the cluster coefficients and Fig. 2(c) is used for the states onto which the Schrödinger equation (2.13) is projected. The corresponding results for the monoexcited  $LS$ -coupled states and cluster coefficients are given in the Appendix.

### V. COUPLED-CLUSTER EQUATIONS FOR ATOMIC SYSTEMS

We now derive the explicit form of the  $LS$ -coupled CPMET equations for closed-shell atomic systems, in terms of the  $LS$ -coupled cluster coefficients (4.18b), by projecting the Schrödinger equation (2.13) onto the  $LS$ -coupled biexcited states (4.10b).

In general, we can conveniently express the left-hand side of (2.13) as a sum of  $i$ -fold excited contributions:

$$(H_N e^T)_e |\Phi\rangle = \sum_{i=0}^N H_e^{(i)} |\Phi\rangle. \quad (5.1)$$

From the diagrammatic point of view this is a sum of all connected resulting skeletons ( $R$  skeletons, cf. Refs. 2 and 15) having  $i$  open paths,  $i = 0, \dots, N$ .

Thus, if we project (2.13) onto the unnormalized  $LS$ -coupled monoexcited states (4.10a), biexcited states (4.10b), and  $|\Phi\rangle$ , we obtain the following system of coupled-cluster equations:

$$\left\langle \begin{array}{c} \bar{n}_1 \bar{l}_1 \\ \bar{n}_1 \bar{l}_1 \end{array} \middle| H_e^{(1)} \middle| \Phi \right\rangle = \sum_{j=0}^2 \langle \bar{n}_1 \bar{l}_1 | \Lambda^{1,j}(0) | \bar{n}_1 \bar{l}_1 \rangle = 0, \quad (5.2a)$$

$$\begin{aligned} N^{-1} \bar{n}_1 \bar{l}_1 \left\langle \begin{array}{c} \bar{L}_i \bar{S}_i (\bar{n} \bar{l})^{12} \\ (\bar{n} \bar{l})_{12} \end{array} \middle| H_e^{(2)} \middle| \Phi \right\rangle \\ = \sum_{j=0}^2 \langle \langle \bar{n} \bar{l} \rangle^{12} | \Lambda^{2,j}(\bar{L}_i \bar{S}_i) | (\bar{n} \bar{l})_{12} \rangle = 0, \quad (5.2b) \end{aligned}$$

and the equation

$$\langle \Phi | H_{\mathbf{e}}^{(0)} | \Phi \rangle = \sum_{j=1}^2 \Lambda^{0,j} = \Delta\epsilon_1 + \Delta\epsilon_2 = \Delta\epsilon \quad (5.3)$$

determining the correlation energy in terms of the monoexcited and biexcited cluster coefficients (cf. Sec. IV of Ref. 14). The CPMET equations are obtained by taking into account only the terms  $\Lambda^{2,0}$  and  $\Lambda^{2,2}$  in (5.2b) and the term  $\Lambda^{0,2}$  in (5.3). The remaining terms in (5.2) and (5.3) describe the effect of the monoexcited clusters in the ECPMET approximation  $T \approx T_1 + T_2$ , which includes in (5.2) only those terms which are linear in the monoexcited cluster coefficients ( $\Lambda^{1,1}$  and  $\Lambda^{2,1}$ ). The terms  $\Lambda^{1,2}$  and  $\Lambda^{2,1}$  describe the interaction between the monoexcited and biexcited clusters. Finally, we note that

$$\Lambda^{2,2} = \Lambda_L^{2,2} + \Lambda_{NL}^{2,2}, \quad (5.4)$$

where the subscripts  $L$  and  $NL$  refer to the linear and nonlinear (quadratic) terms in the biexcited cluster coefficients. The latter arise from the disconnected tetraexcited component  $\frac{1}{2}T_2^2$  in (2.11a). We now derive the explicit form of the  $LS$ -coupled CPMET equations from (5.2) and (5.3). The additional terms which are needed to describe the effect of the monoexcited clusters are given in the Appendix.

#### A. Orbital angular momentum diagrams for CPMET

In order to extend the spin-symmetry-adapted CPMET results of Refs. 13 and 14 to the  $LS$ -coupled case for atomic systems, it is only necessary to construct the orbital angular momentum diagrams corresponding to the orbital Brandow diagrams which represent the contributions to the various terms in (5.2) and (5.3). These orbital diagrams and the rules for constructing them have been given elsewhere<sup>13</sup> for the spin-symmetry-adapted case. For convenience, we list the orbital diagrams in Fig. 3, using labeling schemes appropriate to the atomic case. Thus, Fig. 3(a) corresponds to the absolute term  $\Lambda^{2,0}$  in (5.2b), Fig. 3(b) gives the contributions to the linear term  $\Lambda_L^{2,2}$  in (5.2b), and Fig. 3(c) gives the contributions to the nonlinear term  $\Lambda_{NL}^{2,2}$ . Finally, Fig. 3(d) gives the correlation energy contribution  $\Delta\epsilon_2$  in (5.3). The various diagrams are distinguished using the same labels ( $i_\kappa$ ,  $ii_\kappa$ , etc.) as in Fig. 3 of Ref. 13. In our case each Brandow  $T_2$  vertex defines an  $LS$ -coupled biexcited cluster coefficient (4.18b) and the labels on the external lines correspond to those defining the bra state in (5.2b). In general, we use tildes to distinguish the fixed labels [those in (5.2b)] from the untilded or summation labels.

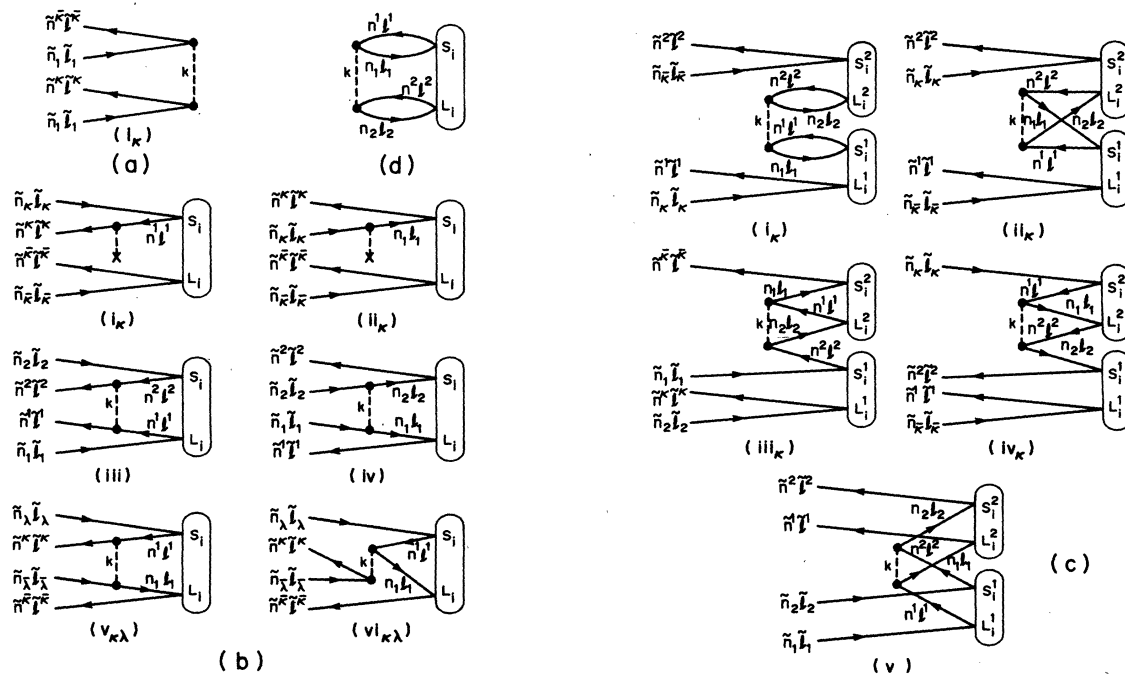


FIG. 3. Orbital (radial) Brandow CPMET diagrams for the  $LS$ -coupled case associated with the terms  $\Lambda^{2,0}$  (a),  $\Lambda_L^{2,2}$  (b),  $\Lambda_{NL}^{2,2}$  (c),  $\Lambda^{0,2}$  (d) given in Eqs. (5.11a), (5.11b), (5.11c), and (5.12), respectively (cf. Sec. V for further details).



The orbital angular momentum diagram associated with each orbital diagram in Fig. 3 is constructed using the rules given in Ref. 13 for the construction of the spin diagram except that we now use the diagrams of Fig. 1(a) and Fig. 1(b) for the  $V$  and  $F$  vertices. Thus, by using Fig. 2(c) for the angular part of the bra state in (5.2b), Figs. 1(a) or 1(b) for the interaction part, and 2(b) for the angular part of each Brandow  $T_2$  vertex, Fig. 2(a), we can construct the resulting orbital angular momentum diagram for each orbital diagram in Fig. 3. These diagrams are given in Fig. 4 where Fig. 4(a) corresponds to Fig. 3(a), etc. In particular, we note that both diagrams ( $i_\kappa$ ) and ( $ii_\kappa$ ) in Fig. 3(b) have the same orbital angular momentum diagram, Fig. 4(b) ( $i_\kappa, ii_\kappa$ ). For the associated spin diagrams we refer to Fig. 5 of Ref. 13. It is interesting to note that these spin diagrams can be easily obtained from the orbital angular momentum diagrams: simply remove the interaction line  $k$  and its end vertices and replace all labels by the corresponding spin labels ( $l_1, l_1 \rightarrow \frac{1}{2}, L_i \rightarrow S_i$ , etc.). Thus, for example, Fig. 4(a) reduces to Fig. 5(a) of Ref. 13 and gives the spin factor in Table I of Ref. 13.

The algebraic expressions (orbital angular momentum factors) corresponding to each diagram of Fig. 4 can be evaluated using the graphical methods of spin algebras (for a concise summary see Appendix I of Ref. 18). Thus, the contributions of Figs. 4(a) and 4(d) are directly proportional to a 6- $j$  coefficient. Figure 4(b) ( $i_\kappa, ii_\kappa$ ) can be separated over two lines [rule (70) of Ref. 18] to give

TABLE I. Orbital angular momentum factor obtained from the diagram of Fig. 4(a) for the absolute term  $\Lambda^2, 0$  [Eq. (5.11a)] of the CPMET equations. The corresponding orbital diagram is given in Fig. 3(a).

Orbital angular momentum diagram	Orbital angular momentum factor $\mathcal{L}_1^i$
( $i_\kappa$ )	$p_{\kappa a} F_a \left\{ \begin{matrix} \bar{l}^{\kappa} \bar{l}^{\kappa} L_i \\ \bar{l}_2 \bar{l}_1 k \end{matrix} \right\}$

two "oyster" diagrams [Eq. (74) of Ref. 18]. Similarly Figs. 4(b) ( $iii$ ) and ( $iv$ ) give an oyster and a 6- $j$  symbol and Figs. 4(b) ( $\nu_{\kappa\lambda}$ ) and ( $vi_{\kappa\lambda}$ ) give a product of two 6- $j$  symbols after separation over three lines [rule (71) of Ref. 18].

For the diagrams of Fig. 4(c), corresponding to the nonlinear part of CPMET, the results are more complicated: Fig. 4(c) ( $i_\kappa$ ) can be separated twice over three lines to give a product of three 6- $j$  symbols, Figs. 4(c) ( $iii_\kappa$ ), ( $iv_\kappa$ ), and ( $v$ ) can each be separated twice over two lines to give two oysters and a 6- $j$  symbol. Finally, Fig. 4(c) ( $ii_\kappa$ ) is not separable over two or three lines and gives a genuine 12- $j$  symbol of the first kind which can be evaluated as a single sum over a product of four 6- $j$  symbols using the crossover sum rule (cf. Ref. 17 and Fig. 5 of Ref. 37).

The orbital angular momentum factors obtained from the diagrams of Figs. 4(a)–4(d) are given in Tables I–IV, respectively. The overall factors

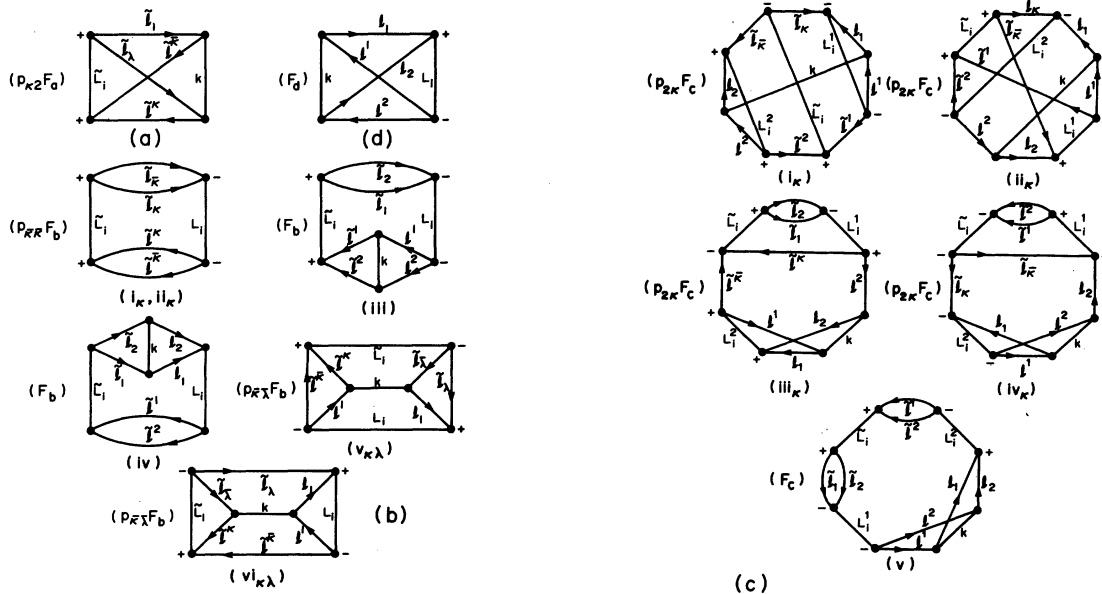


FIG. 4. Orbital angular momentum diagrams corresponding to the orbital diagrams of Fig. 3. The overall factors associated with each diagram are defined in Eqs. (5.5) and (5.6).

TABLE II. Orbital angular momentum factors obtained from the diagrams of Fig. 4(b) for the linear part  $\Lambda_L^{2,2}$  [Eq. (5.11b)] of the CPMET equations. The corresponding orbital diagrams are given in Fig. 3(b).

Orbital angular momentum diagram	$i$	Orbital angular momentum factors $\mathcal{L}_i^{\text{II}}, i=1, \dots, 6$
$(i_\kappa)$	1	$p_{\kappa\kappa}\delta(\tilde{L}_i, L_i)$
$(ii_\kappa)$	2	$p_{12}\delta(\tilde{L}_i, L_i) \left\{ \begin{matrix} \tilde{l}^1 \tilde{l}^2 \tilde{L}_i \\ l^2 l^1 k \end{matrix} \right\}$
$(iii)$	3	$p_{21}\delta(\tilde{L}_i, L_i) \left\{ \begin{matrix} \tilde{l}_1 \tilde{l}_2 \tilde{L}_i \\ l_2 l_1 k \end{matrix} \right\}$
$(iv)$	4	$p_{\kappa\lambda} F_b \left\{ \begin{matrix} \tilde{l}_\kappa k l_1 \\ L_i \tilde{l}_\lambda \tilde{L}_i \end{matrix} \right\} \left\{ \begin{matrix} \tilde{l}^\kappa k l^1 \\ L_i \tilde{l}^\kappa \tilde{L}_i \end{matrix} \right\}$
$(vi_{\kappa\lambda})$	5	$p_{\bar{\kappa}\lambda}(-1)^{\tilde{l}_\lambda + l_1 + L_i} F_b \left\{ \begin{matrix} \tilde{l}^\kappa \tilde{l}^\kappa \tilde{L}_i \\ \tilde{l}_\lambda \tilde{l}_\lambda k \end{matrix} \right\} \left\{ \begin{matrix} l^1 \tilde{l}^\kappa L_i \\ \tilde{l}_\lambda l_1 k \end{matrix} \right\}$

associated with these diagrams are

$$F_a = [\tilde{L}_i]^{1/2}, \quad (5.5a)$$

$$F_b = [\tilde{L}_i, L_i]^{1/2}, \quad (5.5b)$$

$$F_c = [\tilde{L}_i, L_i^1, L_i^2]^{1/2}, \quad (5.5c)$$

$$F_d = [L_i]^{1/2}, \quad (5.5d)$$

$$p_{ij} = (-1)^{i\tilde{\phi}^{12} + j\tilde{\phi}_{12}}, \quad (5.6)$$

where  $\tilde{\phi}^{12}$ ,  $\tilde{\phi}_{12}$  are defined as in (4.14), except that tilded angular momenta are used. Finally, the 12- $j$  symbol of the first kind appearing in Table III can be expressed as

$$\left\{ \begin{matrix} j_1 j_2 j_3 j_4 \\ k_1 k_2 k_3 k_4 \\ l_1 l_2 l_3 l_4 \end{matrix} \middle| 1 \right\} = \sum_X (-1)^{R_4 - X} [X] \left\{ \begin{matrix} j_1 k_1 X \\ k_1 j_2 l_1 \end{matrix} \right\} \left\{ \begin{matrix} j_2 k_2 X \\ k_3 j_3 l_2 \end{matrix} \right\} \\ \times \left\{ \begin{matrix} j_3 k_3 X \\ k_4 j_4 l_3 \end{matrix} \right\} \left\{ \begin{matrix} j_4 k_4 X \\ j_1 k_1 l_4 \end{matrix} \right\}, \quad (5.7)$$

where

$$R_4 = \sum_{i=1}^4 (j_i + k_i + l_i). \quad (5.8)$$

TABLE III. Orbital angular momentum factors obtained from the diagrams of Fig. 4(c) for the nonlinear (quadratic) part  $\Lambda_{NL}^{2,2}$  [Eq. (5.11c)] of the CPMET equations. The corresponding orbital diagrams are given in Fig. 3(c).

Orbital angular momentum diagram	$i$	Orbital angular momentum factors $\mathcal{L}_i^{\text{III}}, i=1, \dots, 5$
$(i_\kappa)$	1	$p_{2\bar{\kappa}}(-1)^{\tilde{l}^2 + l_2 + i_\kappa} F_c \left\{ \begin{matrix} l^1 \tilde{l}^1 L_i^1 \\ \tilde{l}_\kappa l_1 k \end{matrix} \right\} \left\{ \begin{matrix} l^2 \tilde{l}^2 L_i^2 \\ \tilde{l}_\kappa l_2 k \end{matrix} \right\} \left\{ \begin{matrix} \tilde{l}^1 \tilde{l}^2 \tilde{L}_i \\ \tilde{l}_\kappa \tilde{l}_\kappa k \end{matrix} \right\}$
$(ii_\kappa)$	2	$p_{2\kappa}(-1)^{\tilde{l}^1 + \tilde{l}_\kappa + k + \tilde{L}_i + L_i^1 + L_i^2} F_c \left\{ \begin{matrix} \tilde{l}^1 \tilde{l}^2 \tilde{l}^2 l_2 \\ \tilde{L}_i L_i^2 k L_i^1 \\ \tilde{l}_\kappa \tilde{l}_\kappa l_1 l^1 \end{matrix} \middle  1 \right\}$
$(iii_\kappa)$	3	$p_{\kappa 2}(-1)^{l^1 + l_2 + L_i^2} \delta(\tilde{L}_i, L_i^1) \delta(l^2, \tilde{l}^\kappa) [\tilde{l}^\kappa]^{-1} [L_i^2]^{1/2} \left\{ \begin{matrix} l^1 l^2 L_i^2 \\ l_2 l_1 k \end{matrix} \right\}$
$(iv_\kappa)$	4	$p_{2\kappa}(-1)^{l^1 + l_2 + L_i^2} \delta(\tilde{L}_i, L_i^1) \delta(l_2, \tilde{l}_\kappa) [\tilde{l}_\kappa]^{-1} [L_i^2]^{1/2} \left\{ \begin{matrix} l^1 l^2 L_i^2 \\ l_2 l_1 k \end{matrix} \right\}$
$(v)$	5	$\delta(\tilde{L}_i, L_i^1) \delta(\tilde{L}_i, L_i^2) [\tilde{L}_i]^{-1/2} \left\{ \begin{matrix} l^1 l^2 \tilde{L}_i \\ l_2 l_1 k \end{matrix} \right\}$

TABLE IV. Spin factor  $S_1^{IV}$  and orbital angular momentum factor  $\mathcal{L}_1^{IV}$  for the correlation energy  $\Delta\epsilon_2$  [Eq. (5.12)] of CPMET. The orbital and orbital angular momentum diagrams are given in Figs. 3(d) and 4(d), respectively.

Spin factor $S_1^{IV}$	Orbital angular momentum factor $\mathcal{L}_1^{IV}$
$(-1)^{1+S_i} [S_i]^{1/2}$	$F_d \left\{ \begin{array}{l} l^1 l^2 L_i \\ l_2 l_1 k \end{array} \right\}$

### B. *LS*-coupled CPMET equations

Using the rules of Ref. 13, 14, 16, and 17 we find that each diagram of Fig. 3 gives an algebraic contribution having the general form

$$\sum_{\{\kappa\lambda\}} \sum_{\{LS\}} \sum_k \sum_{\{nl\}} \mathcal{L} S \mathcal{O} \quad (5.9)$$

where  $\mathcal{L}$  and  $S$  are the orbital angular momentum and spin factors, respectively, and

$$\mathcal{O} = (-1)^{l+h+p} w \mathfrak{M} \mathcal{T} \quad (5.10)$$

is the orbital factor consisting of an orbital phase factor, a topological or weight factor  $w$  (cf. Ref. 13), a radial  $f$  or  $v$  matrix element  $\mathfrak{M}$  and 0, 1, or 2 biexcited cluster coefficients  $\mathcal{T}$ . The spin and orbital factors corresponding to the orbital

TABLE V. Spin factors and orbital angular momentum factors for the term  $\Lambda^{1,2}$  [Eq. (A1c)].

Spin factor $S_i^V, i=1,2,3.$	Orbital angular momentum factor $\mathcal{L}_i^V, i=1,2,3.$
$(-1)^{1+S_i} ([S_i]/2)^{1/2}$	$G_c \left\{ \begin{array}{l} l_1 l_2 L_i \\ \bar{l} l_1 k \end{array} \right\}$
$(-1)^{1+S_i} ([S_i]/2)^{1/2}$	$G_c \left\{ \begin{array}{l} l^1 l^2 L_i \\ \bar{l} l_1 k \end{array} \right\}$
$(-1)^{1+S_i} ([S_i]/2)^{1/2}$	$G_c (-1)^{l+\bar{l}+L_i}$

angular momentum factors of Tables I–III are given in Tables I–III, respectively, of Ref. 13. In our case the orbital factors are simply obtained from those of Ref. 13 by (i) replacing the  $f$  and  $v$  matrix elements by the corresponding radial ones (3.16) and (3.6), (ii) replacing each spin-symmetry-adapted  $\tau_2$  cluster coefficient by the corresponding *LS*-coupled one (4.18b) using the labeling schemes given on the diagrams in Fig. 3, and (iii) summing over all internal line labels  $\{[nl]\}$  in (5.9), all quantum numbers inside the ovals of the Brandow  $T_2$  vertices  $\{[LS]\}$  in (5.9), the quantum number  $k$  and the indices  $\kappa, \lambda$ , if present, which index the various external line labeling schemes [cf. Eq. (4.12)].

Thus, we obtain the following results for the terms in (5.2b) which define the *LS*-coupled CPMET equations:

$$\langle (\bar{n}\bar{l})^{12} | \Lambda^{2,0}(\bar{L}_i, \bar{S}_i) | (\bar{n}\bar{l})_{12} \rangle = \sum_{\kappa=1}^2 \sum_k (-1)^\kappa \mathfrak{X}(I, 1) X^k(\bar{\kappa}_p \bar{l}_h | \bar{\kappa}_p \bar{2}_h), \quad (5.11a)$$

$$\begin{aligned} \langle (\bar{n}\bar{l})^{12} | \Lambda_L^{2,2}(\bar{L}_i, \bar{S}_i) | (\bar{n}\bar{l})_{12} \rangle &= \sum_{\kappa=1}^2 \sum_{L_i \bar{S}_i} \left( \sum_{1_p} \delta(l^1, \bar{l}^\kappa) \mathfrak{X}(II, 1) \langle \bar{\kappa}_p | f | 1_p \rangle [1 \bar{\kappa} || \bar{\kappa} \bar{\kappa}] - \sum_{1_h} \delta(l_1, \bar{l}_\kappa) \mathfrak{X}(II, 2) \langle 1_h | f | \bar{\kappa}_h \rangle [\bar{\kappa} \bar{\kappa} || 1 \bar{\kappa}] \right) \\ &+ \sum_{L_i \bar{S}_i} \sum_k \left( \sum_{1_p 2_p} \mathfrak{X}(II, 3) X^k(\bar{l}_p 1_p | \bar{2}_p 2_p) [12 || \bar{1} \bar{2}] + \sum_{1_h 2_h} \mathfrak{X}(II, 4) X^k(1_h \bar{l}_h | 2_h \bar{2}_h) [\bar{1} \bar{2} || 12] \right) \\ &+ \sum_{\kappa, \lambda=1}^2 \sum_{1_p 1_h} (-1)^{\kappa+\lambda+1} [\mathfrak{X}(II, 5) X^k(\bar{\kappa}_p 1_p | 1_h \bar{\lambda}_h) - \mathfrak{X}(II, 6) X^k(\bar{\kappa}_p \bar{\lambda}_h | 1_h 1_p)] [1 \bar{\kappa} || \bar{\lambda} 1], \end{aligned} \quad (5.11b)$$

$$\begin{aligned} \langle (\bar{n}\bar{l})^{12} | \Lambda_{NL}^{2,2}(\bar{L}_i, \bar{S}_i) | (\bar{n}\bar{l})_{12} \rangle &= \sum_{L_i^1 \bar{S}_i^1} \sum_{L_i^2 \bar{S}_i^2} \sum_k \sum_{1_h 2_h} \sum_{1_p 2_p} X^k(1_h 1_p | 2_h 2_p) \\ &\times \left( \sum_{\kappa=1}^2 (-1)^\kappa \mathfrak{X}(III, 1) [\bar{1} 1 || \bar{\kappa} 1]_1 [\bar{2} 2 || \bar{\kappa} 2]_2 + \mathfrak{X}(III, 2) [\bar{1} 1 || \bar{\kappa} 2]_1 [\bar{2} 2 || \bar{\kappa} 1]_2 \right. \\ &\quad \left. - \mathfrak{X}(III, 3) [2 \bar{\kappa} || \bar{1} \bar{2}]_1 [\bar{\kappa} 1 || 12]_2 - \mathfrak{X}(III, 4) [\bar{2} \bar{2} || \bar{\kappa} 2]_1 [12 || \bar{\kappa} 1]_2 \right) \\ &+ \frac{1}{2} \mathfrak{X}(III, 5) [12 || \bar{1} \bar{2}]_1 [\bar{1} \bar{2} || 12]_2. \end{aligned} \quad (5.11c)$$

TABLE VI. Spin factors and orbital angular momentum factors for the term  $\Lambda^{2,1}$  [Eq. (A1d)].

Spin factor $S_i^{VI}, i=1,2.$	Orbital angular momentum $\mathcal{L}_i^{VI}, i=1,2.$
$(-1)^{(\kappa+\lambda+1)(1+\tilde{S}_i)}([\tilde{S}_i/2])^{1/2}$	$p_{\kappa\lambda}G_d^1 \begin{Bmatrix} \tilde{l}_\kappa \tilde{l}_\lambda \tilde{L}_i \\ \tilde{l}_\lambda \tilde{l}_\kappa k \end{Bmatrix}$
$(-1)^{(\kappa+\lambda+1)(1+\tilde{S}_i)}([\tilde{S}_i/2])^{1/2}$	$p_{\lambda\kappa}G_d^2 \begin{Bmatrix} \tilde{l}_\lambda \tilde{l}_\kappa \tilde{L}_i \\ \tilde{l}_\kappa \tilde{l}_\lambda k \end{Bmatrix}$

Finally, from Table IV the correlation energy is given by

$$\Delta\epsilon_2 = \frac{1}{2} \sum_{L_i S_i} \sum_h \sum_{h^2 h^1 p^2 p} \mathcal{X}(IV, 1) X^h(1_h 1_p | 2_h 2_p) [12 || 12]. \quad (5.12)$$

In Eqs. (5.11) and (5.12) we are using the notation

$$\mathcal{X}(K, k) = \mathcal{L}_k^K S_k^K \quad (\mathcal{X} = I, II, \dots; k = 1, 2, \dots) \quad (5.13)$$

to refer to the orbital angular momentum factor  $\mathcal{L}_k^K$  in line  $k$  of Table  $K$  and similarly for the spin factor  $S_k^K$  in Table IV and in Tables I–III of Ref. 1. We note that  $\mathcal{L}_1^{II} = \mathcal{L}_2^{II}$ ,  $S_1^{II} = \dots = S_2^{II}$ , and  $S_3^{III} = S_4^{III}$ . We are also using the simplified notation  $i_p = n^i l^i$ ,  $i_h = n_i l_i$ ,  $\tilde{i}_p = \tilde{n}^i \tilde{l}^i$ , etc., where the subscripts  $p$  and  $h$  refer to particle and hole state labels, respectively. Moreover, in the  $\tau_2$  or  $t_2$  matrix elements the  $p, h$  subscripts are dropped since the bra part always contains particle labels and the ket part always contains hole labels. Thus, we have used, for example, the notation

$$[ij||rs] = \langle n^i l^i n^j l^j | \tau_2(L_i, S_i) | n_r l_r n_s l_s \rangle, \quad (5.14a)$$

$$[\tilde{i}\tilde{k}||\tilde{j}\tilde{k}]_r = \langle n^i l^i \tilde{n}^k \tilde{l}^k | \tau_2(L_i^r, S_i^r) | n_j l_j \tilde{n}_r \tilde{l}_r \rangle, \quad r = 1, 2. \quad (5.14b)$$

Thus, (5.11a), (5.11b), and (5.11c) are the absolute, linear, and nonlinear terms, respectively, which after substitution in (5.26), give the system of nonlinear algebraic CPMET equations defining the  $LS$ -coupled  $\tau_2$  cluster coefficients. After solving this system, the correlation energy can be obtained from (5.12). The additional terms needed to account for the monoexcited cluster coefficients are given in the Appendix.

## VI. DISCUSSION

We have derived the orthogonally spin- and orbital-symmetry-adapted ( $LS$ -coupled) coupled-cluster equations for closed-shell atomic systems in explicit form for the mono-excited and bi-excited cluster coefficients starting from our previous results for the spin-symmetry-adapted case, and using techniques based on second quantization and the graphical methods of spin algebras.

The results which we have obtained in Eqs. (5.2), (5.3), (5.11), (5.12) and the Appendix have been recently applied to a correlation energy study and pair energy analysis of Be.<sup>29</sup> We note that for Be the  $LS$ -coupled CPMET equations simplify considerably and for this case we have also considered the additional terms involving the triexcited cluster coefficients which have been derived in Ref. 14 for the spin-symmetry-adapted case. In addition we have also considered various CEPA-type approximations based on the  $LS$ -coupled CPMET equations. These equations and the numerical CPMET- and CEPA-type results will be presented in subsequent papers.

## ACKNOWLEDGMENTS

This work was supported by Natural Sciences and Engineering Research Council of Canada Grants-in-Aid of Research, which are hereby gratefully acknowledged. One of us (B.G.A.) would also like to acknowledge the receipt of an NSERC University Research Fellowship, 1980–1983.

## APPENDIX: MONOEXCITED CLUSTER CONTRIBUTIONS

In order to consider the effect of the monoexcited clusters we consider, in addition to the CPMET equations of Sec. V, the system (5.2a) in which all  $t_1$  cluster coefficients (4.18a) appear linearly, the linear term  $\Lambda^{2,1}$  in (5.2b) which couples (5.2a) and (5.2b), and the additional term  $\Lambda^{0,1}$  for the correlation energy, which in general contains contributions linear and quadratic in the  $t_1$  cluster coefficients. The unlinked cluster components in (2.11a), such as  $\frac{1}{2} T_1^2$  and  $T_1 T_2$ , are neglected.

The pertinent terms in (5.2) are given by

$$\langle \tilde{n}^i \tilde{l}^i | \Lambda^{1,0}(0) | \tilde{n}_i \tilde{l}_i \rangle = \sqrt{2} [\tilde{l}^i]^{1/2} \langle \tilde{n}^i \tilde{l}^i | f | \tilde{n}_i \tilde{l}_i \rangle, \quad (A1a)$$

$$\begin{aligned} \langle \tilde{n}^i \tilde{l}^i | \Lambda^{1,1}(0) | \tilde{n}_i \tilde{l}_i \rangle &= \sum_{n_1} \langle \tilde{n}^i \tilde{l}^i | f | n^i l^i \rangle \langle n^i l^i | t_1(0) | \tilde{n}_i \tilde{l}_i \rangle - \sum_{n_1} \langle n_i \tilde{l}^i | f | \tilde{n}_i \tilde{l}_i \rangle \langle \tilde{n}^i \tilde{l}^i | t_1(0) | n_i l^i \rangle \\ &+ \sum_{in^1 n_1} [2X^0(\tilde{n}^i \tilde{l}_i \tilde{n}_i \tilde{l}_i | n_i l_i n^i l^i) - \sum_k [\tilde{l}^i, l^i]^{-1/2} X^k(\tilde{n}^i \tilde{l}_i n^i l^i | n_i l_i \tilde{n}_i \tilde{l}_i)] \langle n^i l^i | t_1(0) | n_i l^i \rangle, \end{aligned} \quad (A1b)$$

$$\begin{aligned} \langle \bar{n}^1 \bar{l} | \Lambda^{1/2}(0) | \bar{n}_1 \bar{l} \rangle = & - \sum_{L_i S_i} \sum_k \sum_{n^1 l^1 n_1 l_1} \left( \sum_{n_2 l_2} \mathcal{X}(V, 1) X^k(n_1 l_1 n^1 l^1 | n_2 l_2 \bar{n}_1 \bar{l}) \langle n^1 l^1 \bar{n}^1 \bar{l} | \tau_2(L_i, S_i) | n_1 l_1 n_2 l_2 \rangle \right. \\ & \left. - \sum_{n_2 l_2} \mathcal{X}(V, 2) X^k(\bar{n}^1 \bar{l} n^2 l^2 | n_1 l_1 n^1 l^1) \langle n^1 l^1 n^2 l^2 | \tau_2(L_i, S_i) | n_1 l_1 \bar{n}_1 \bar{l} \rangle \right) \\ & + \sum_{L_i S_i} \sum_{l n^1 n_1} \mathcal{X}(V, 3) \langle n_1 l | f | n^1 l \rangle \langle n^1 l^1 \bar{n}^1 \bar{l} | \tau_2(L_i, S_i) | n_1 l n^1 \bar{l} \rangle, \end{aligned} \quad (\text{A1c})$$

$$\begin{aligned} \langle (\bar{n}^1 \bar{l})^{12} | \Lambda^{2/2}(\bar{L}_i, \bar{S}_i) | (\bar{n}^1 \bar{l})_{12} \rangle = & \sum_{\kappa, \lambda=1}^2 \sum_k (-1)^{\kappa+\lambda+1} \\ & \times \left( \sum_{n_1} \mathcal{X}(VI, 1) X^k(n_1 \bar{l}^{\kappa} \bar{n}_\lambda \bar{l}_\lambda | \bar{n}^{\kappa} \bar{l}^{\kappa} \bar{n}_\lambda \bar{l}_\lambda) \langle \bar{n}^{\kappa} \bar{l}^{\kappa} | t_1(0) | n_1 \bar{l}^{\kappa} \rangle \right. \\ & \left. - \sum_{n_1} \mathcal{X}(VI, 2) X^k(\bar{n}^{\lambda} \bar{l}^{\lambda} n^1 \bar{l}_\kappa | \bar{n}^{\lambda} \bar{l}^{\lambda} \bar{n}_\kappa \bar{l}_\kappa) \langle n^1 \bar{l}_\kappa | t_1(0) | \bar{n}_\kappa \bar{l}_\kappa \rangle \right), \end{aligned} \quad (\text{A1d})$$

$$\begin{aligned} \Delta \epsilon_i = & \sqrt{2} \sum_{l n^1 n_1} [l]^{1/2} \langle n_1 l | f | n^1 l \rangle \langle n^1 l | t_1(0) | n_1 l \rangle \\ & + \frac{1}{2} \sum_{l^1 n^1 n_1} \sum_{l^2 n^2 n_2} \left( 2X^0(n_1 l^1 n^1 l^1 | n_2 l^2 n^2 l^2) - \sum_k [l^1, l^2]^{-1/2} X^k(n_1 l^1 n^2 l^2 | n_2 l^2 n^1 l^1) \right) \\ & \times \langle n^1 l^1 | t_1(0) | n_1 l^1 \rangle \langle n^2 l^2 | t_1(0) | n_2 l^2 \rangle. \end{aligned} \quad (\text{A2})$$

In (A1c) and (A1d) the orbital angular momentum and spin factors  $\mathcal{L}_i^K$ ,  $S_i^K$ , are given in line  $i$  of Table  $K$ . The overall factors appearing in Tables V and VI are defined by

$$G_a = [\bar{l}]^{-1/2}, \quad (\text{A3a})$$

$$G_b^1 = [\bar{l}]^{-1}, \quad G_b^2 = [\bar{l}, l]^{-1/2}, \quad (\text{A3b})$$

$$G_c = ([L_i] / [\bar{l}])^{1/2} \quad (\text{A3c})$$

$$G_d^1 = ([\bar{L}_i] / [\bar{l}^{\kappa}])^{1/2}, \quad G_d^2 = ([\bar{L}_i] / [\bar{l}_\kappa])^{1/2}, \quad (\text{A3d})$$

$$G_e^1 = [l]^{-1/2}, \quad G_e^2 = [l^1, l^2]^{-1/2} \quad (\text{A3e})$$

and the phase factor  $p_{ij}$  is defined in (5.6). Finally, we note that in the HF case the right-hand side of (A1a), the final term in (A1c) and the first term in (A2) vanish.

\*Also at the Department of Chemistry and Guelph-Waterloo Center for Graduate Work in Chemistry, Waterloo Campus, University of Waterloo, Waterloo, Ontario, Canada.  
<sup>1</sup>F. Coster, Nucl. Phys. **7**, 421 (1958); F. Coster and H. Kümmel, *ibid.* **17**, 477 (1960); H. Kümmel, in *Lectures on the Many-Body Problem*, edited by E. R. Caianiello (Academic, New York, 1962), p. 265.  
<sup>2</sup>J. Čížek, J. Chem. Phys. **45**, 4256 (1966); Adv. Chem. Phys. **14**, 35 (1969).  
<sup>3</sup>J. A. Pople, R. Krishnan, H. B. Schlegel, and J. S. Binkley, Int. J. Quantum Chem. **14**, 545 (1978).  
<sup>4</sup>R. J. Bartlett and G. D. Purvis, Int. J. Quantum Chem. **14**, 561 (1978); Phys. Scr. **21**, 255 (1980).  
<sup>5</sup>I. Lindgren and S. Salomonson, Phys. Scr. **21**, 335 (1980).  
<sup>6</sup>J. Čížek and J. Paldus, Int. J. Quantum Chem. **5**, 359 (1971).  
<sup>7</sup>F. E. Harris, in *Electrons in Finite and Infinite Structures*, edited by P. Phariseau and L. Schiere (Plenum, New York, 1977), p. 274.  
<sup>8</sup>A. C. Hurley, *Electron Correlation in Small Molecules*

(Academic, New York, 1976).

<sup>9</sup>W. Kutzelnigg, in *Modern Theoretical Chemistry*, edited by H. F. Schaefer III (Plenum, New York, 1977), p. 129.  
<sup>10</sup>H. Kümmel, K. H. Lührmann, and J. G. Zabolitsky, Phys. Rep. **36**, 1 (1978).  
<sup>11</sup>I. Lindgren and J. Morrison, *Atomic Many-Body Theory* (Springer, Berlin, to be published).  
<sup>12</sup>J. Čížek and J. Paldus, Phys. Scr. **21**, 251 (1980). The most recent review of molecular applications may be found in R. J. Bartlett, Ann. Rev. Phys. Chem. **32** (in press).  
<sup>13</sup>J. Paldus, J. Chem. Phys. **67**, 303 (1977).  
<sup>14</sup>B. G. Adams and J. Paldus, Phys. Rev. A **20**, 1 (1979).  
<sup>15</sup>J. Paldus and J. Čížek, Adv. Quantum Chem. **9**, 105 (1975).  
<sup>16</sup>We are using the graphical methods of Ref. 6. A useful summary is presented in Appendix I of Ref. 7. Other approaches are given in Refs. 8–10 (cf. also the references in Ref. 2).  
<sup>17</sup>E. El Baz and B. Castel, *Graphical Methods of Spin Algebras in Atomic, Nuclear, and Particle Physics*

- (Dekker, New York, 1972).
- <sup>18</sup>J. Paldus, B. G. Adams, and J. Čížek, *Int. J. Quantum Chem.* **11**, 813 (1977).
- <sup>19</sup>A. P. Jucys, I. B. Levinson, and V. V. Vanagas, *Mathematical Apparatus of the Theory of Angular Momentum* (Institute of Physics and Mathematics of the Academy of Sciences of the Lithuanian Soviet Socialist Republic, Mintis, Vilnius, 1960), in Russian (English translations by Israel Program for Scientific Translations, Jerusalem, 1962, and Gordon and Breach, New York, 1964); A. P. Jucys and A. A. Bandzaitis, *The Theory of Angular Momentum in Quantum Mechanics*, 2nd ed. (Mokslas, Vilnius, Lithuania, 1977), in Russian.
- <sup>20</sup>D. M. Brink and G. R. Satchler, *Angular Momentum*, 2nd ed. (Clarendon, Oxford, 1968).
- <sup>21</sup>J. Paldus and M. J. Boyle, *Phys. Rev. A* **22**, 2299 (1980); M. J. Boyle and J. Paldus, *ibid.* **22**, 2316 (1980).
- <sup>22</sup>J. Paldus, J. Čížek, and I. Shavitt, *Phys. Rev. A* **5**, 50 (1972).
- <sup>23</sup>N. W. Winter, A. Laferrière, and W. McKoy, *Phys. Rev. A* **2**, 49 (1970).
- <sup>24</sup>J. Morrison, *J. Phys. (London)* **B6**, 2205 (1973).
- <sup>25</sup>S. Garpman, I. Lindgren, J. Lindgren, and J. Morrison, *Phys. Rev. A* **11**, 758 (1975).
- <sup>26</sup>C. C. J. Roothaan, Lester M. Sachs, and A. W. Weiss, *Rev. Mod. Phys.* **32**, 186 (1960); C. C. J. Roothaan and P. S. Bagus, *Methods Comp. Phys.* **2**, 47 (1963).
- <sup>27</sup>E. Clementi, *IBM J. Res. Dev. Suppl.* **9**, 2 (1965); R. C. Raffanetti, *J. Chem. Phys.* **59**, 5936 (1973) and references therein.
- <sup>28</sup>Carlos F. Bunge, *Phys. Rev.* **168**, 92 (1968); *Phys. Rev. A* **14**, 1965 (1976).
- <sup>29</sup>B. G. Adams, K. Jankowski, and J. Paldus, *Phys. Rev. A* **24**, 2316 (1981); **24**, 2330 (1981).
- <sup>30</sup>We are using the Condon and Shortley phase convention for the spherical harmonics (cf. Ref. 9).
- <sup>31</sup>J. C. Slater, *Quantum Theory of Atomic Structure* (McGraw-Hill, New York, 1960), Vol. II.
- <sup>32</sup>J. C. Slater, *Quantum Theory of Atomic Structure* (McGraw-Hill, New York, 1960), Vol. I; E. U. Condon and G. H. Shortley, *Theory of Atomic Spectra* (Cambridge University Press, Cambridge, 1935).
- <sup>33</sup>Brian L. Silver, *Irreducible Tensor Methods: An Introduction for Chemists* (Academic, New York, 1976); A. R. Edmonds, *Angular Momentum in Quantum Mechanics* (Princeton University Press, Princeton, 1957).
- <sup>34</sup>J. S. Briggs, *Rev. Mod. Phys.* **43**, 189 (1971); P. G. H. Sandars, *Adv. Chem. Phys.* **14**, 365 (1966); V. V. Tolmachev, *ibid.* **14**, 471 (1966).
- <sup>35</sup>E. P. Wigner, in *Quantum Theory of Angular Momentum*, edited by L. C. Biedenharn and H. Van Dam (Academic, New York, 1965).
- <sup>36</sup>This follows from (3.17) and (3.11) and the graphical rules (58') and (66) of Ref. 7.
- <sup>37</sup>J. Paldus and P. E. S. Wormer, *Phys. Rev. A* **18**, 827 (1978).